CERES Angular Distribution Model Working Group Report

Wenying Su

Wenying.Su-1@nasa.gov

NASA LaRC, Hampton VA

Lusheng Liang[1] Zachary Eitzen[2]

Sergio Sejas[2] Victor Sothcott[2]

1. Analytical Mechanics Associates, Inc., Hampton, VA

2. ADNET Systems, Inc., Hampton VA

CERES Science Team Meeting, May 14-16, 2024

NASA Langley Research Center, Hampton, VA

From radiance to flux: angular distribution models

- Sort observed radiances into angular bins over different scene types;
- Integrate radiance over all θ and ϕ to estimate the anisotropic factor for each scene type:

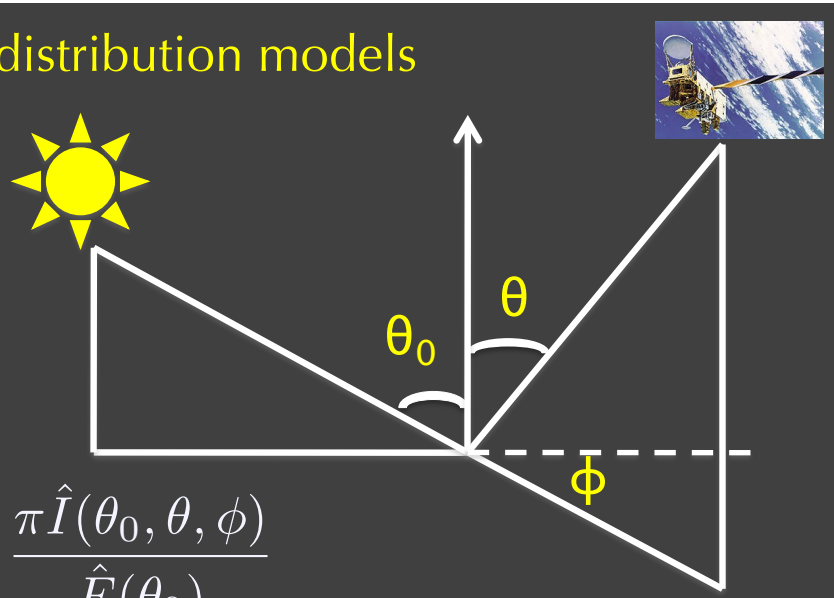

$$R(\theta_0,\theta,\phi)=\frac{\pi\hat{I}(\theta_0,\theta,\phi)}{\int_0^{2\pi}\int_0^{\frac{\pi}{2}}\hat{I}(\theta_0,\theta,\phi)cos\theta sin\theta d\theta d\phi}=\frac{\pi\hat{I}(\theta_0,\theta,\phi)}{\hat{F}(\theta_0)}$$

- For each radiance measurement, first determine the scene type, then apply scene type dependent anisotropic factor to observed radiance to derive TOA flux:

$$F(\theta_0)=\frac{\pi I_o(\theta_0,\theta,\phi)}{R(\theta_0,\theta,\phi)}$$

Outline

- Sensitivity of CERES ADMs to different climate states
- A new method to partition TOA SW fluxes into visible and near-IR fluxes

Sensitivity of CERES ADMs to different climate states

How resilient are ADMs to climate variability and change?

- As the mean climate state shifts, can the Terra/Aqua ADMs constructed using data taken in the early 2000s be used for flux inversion now and in the coming decades?
- Using data taken during different phases of ENSO to test LW ADM sensitivity to climate variability:
  - Use the NOAA Physical Sciences Laboratory Multivariate ENSO Index (MEI) v2 to characterize ENSO phase.
  - A set of "El Niño ADMs" was constructed using 12 months of Terra RAPS data plus 12 months of Terra cross track data with MEI > 0.5.
  - A set of "La Niña ADMs" was constructed using 12 months of Terra RAPS data plus 12 months of Terra cross track data with MEI < -0.5.

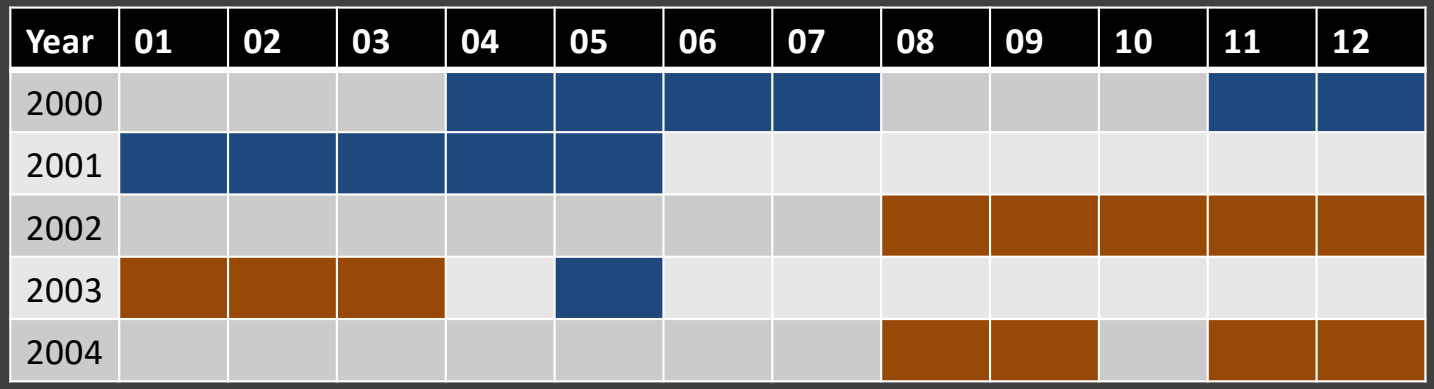

Terra all-sky daytime LW flux difference at the footprint level: El Niño - La Niña ADMs

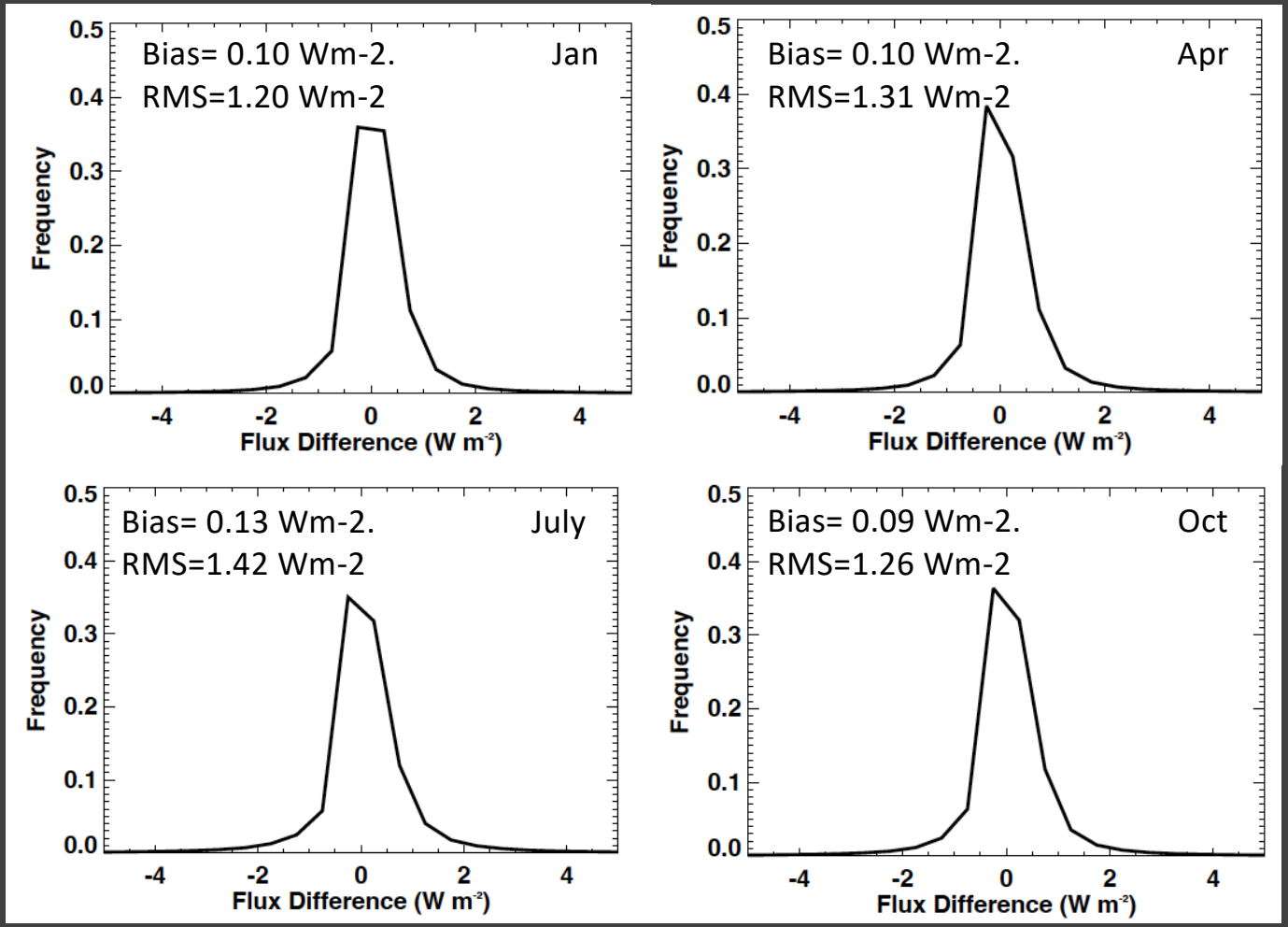

Terra all-sky daytime LW flux difference: El Niño - La Niña ADMs

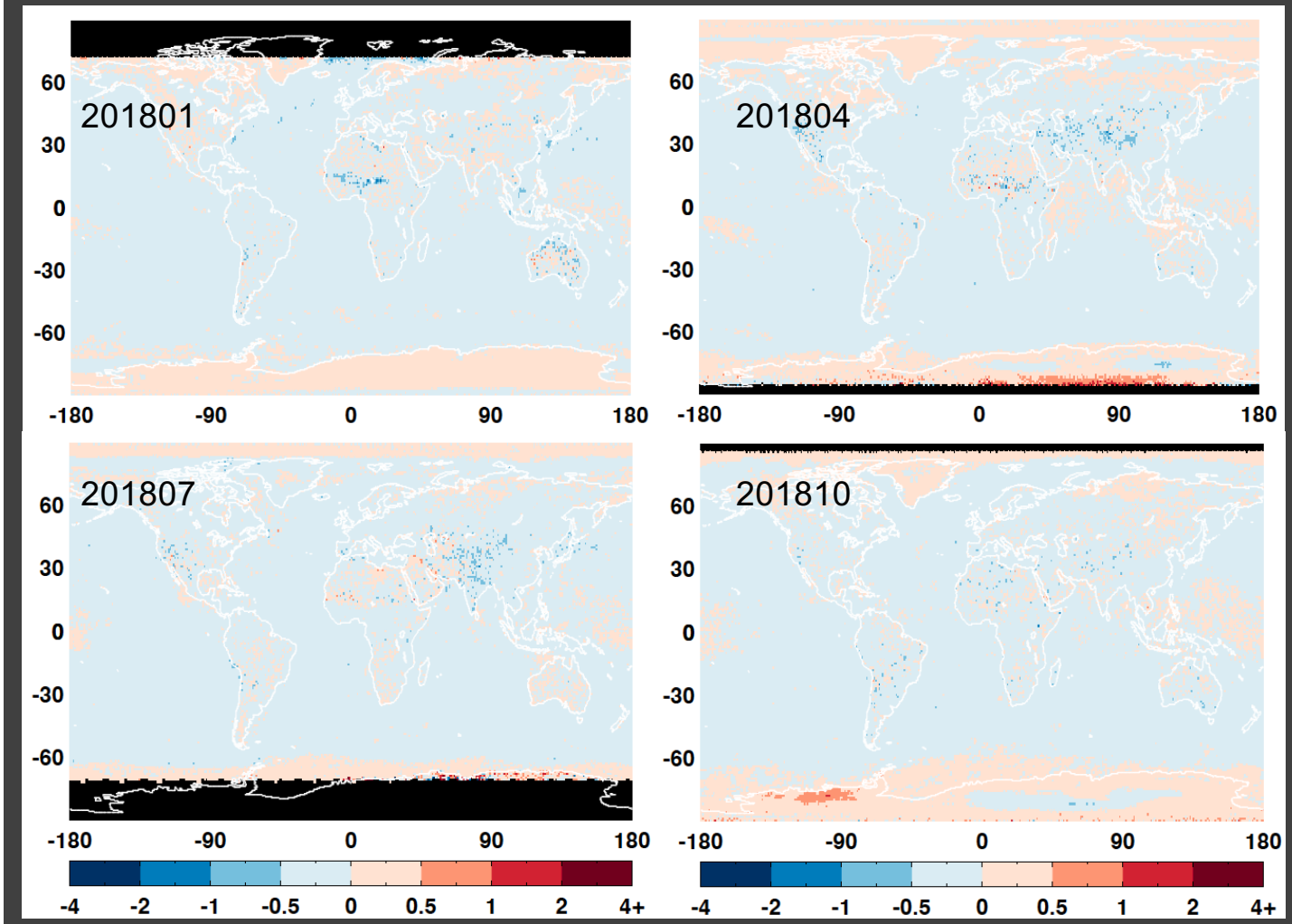

	All-sky bias (W m^{-2}, %)	All-sky RMS
201801	0.13 (0.06%)	1.08 (0.45%)
201804	0.13 (0.05%)	1.17 (0.48%)
201807	0.14 (0.06%)	1.17 (0.47%)
201810	0.12 (0.05%)	1.09 (0.45%)

Developing El Niño and La Niña SW ADMs

- For land/ocean, TRMM scene identification was used for constructing SW ADMs due to limited RAPS data for each set of ADMs:
  - Clear ocean: 4 wind speed bins (quartiles of the ocean wind speed distribution)
  - Cloudy ocean: 2 phases, 12 cloud fraction bins, and 14 cloud optical depth bins
  - Clear land: 4 surface types (mod-hi tree/shrub coverage, low-mod tree/shrub coverage, dark desert and bright desert)
  - Cloudy land: 2 phases, 5 cloud fraction bins, and 6 cloud optical depth bins

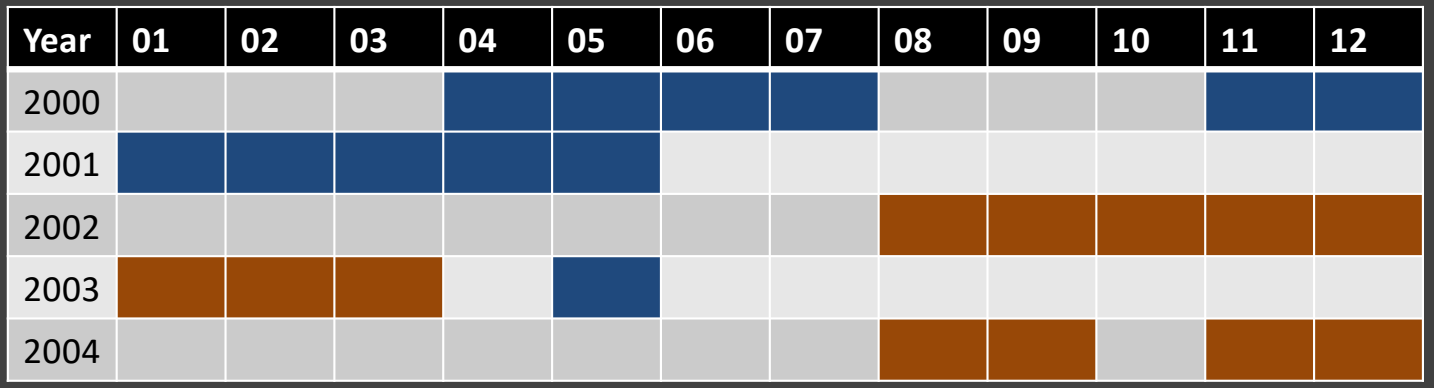

Developing El Niño and La Niña SW ADMs

- To construct SW ADMs over snow/ice, the selection criterion used for land/ocean is not suitable, as one set has more boreal winter data than the other.
- Data selection criterion was modified: MEI<0 for La Niña and MEI>0 for El Niño.
- This criterion was used to select the symmetrically distributed El Niño and La Niña data to construct snow/ice ADMs.
- For snow/ice, modified Ed4 Terra/Aqua scene identification was used:

Fresh Snow	**Clear: 1° regional monthly ADM using Ross-Li 3-para fit for different NDVI (0.1), cosθ (0.2), and surface roughness;**
	Cloudy: function of cloud fraction and snow fraction; for overcast consider surface brightness and cloud optical depth
Perm. Snow	Separate Clear Antarctica and Clear Greenland
	Partly cloudy: 4 cloud fraction bins
	Overcast: cloud phase (2), and log optical depth bin (4)
Sea ice	Clear: sea ice fraction (6), for 100% sea ice coverage use sea ice brightness index (3) to classify surface brightness
	Partly cloudy: cloud fraction (4), for 100% sea ice coverage use sea ice brightness index (3) to classify surface brightness
	Overcast: sea ice brightness index (5), phase (2), linear function of ln(tau)

SW flux differences from these two sets of ADMs show no dependence on the ENSO phase

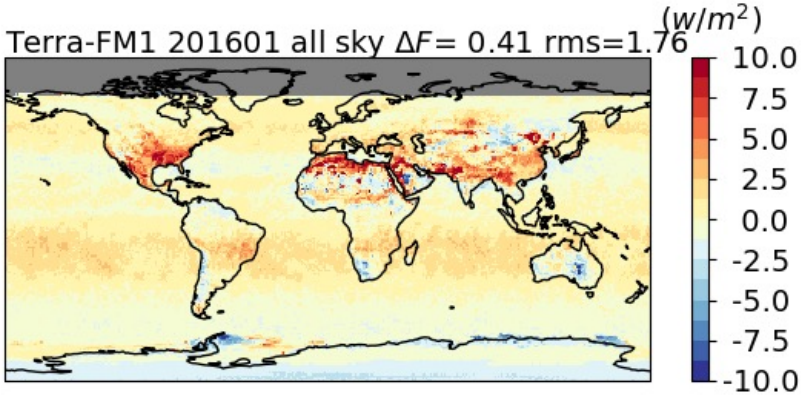

MEI= 2.0

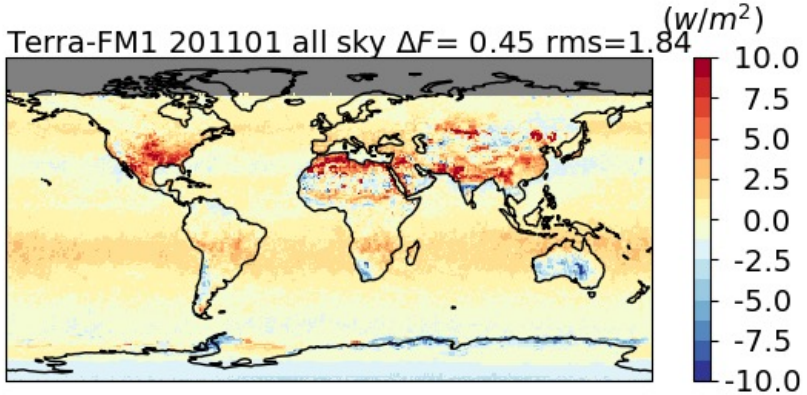

MEI= -1.8

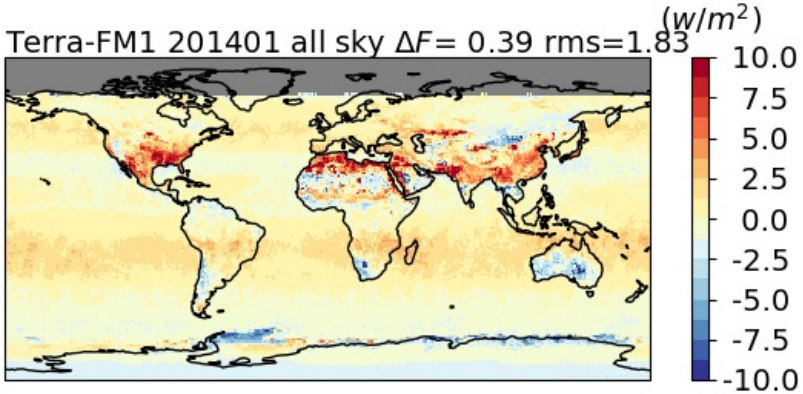

MEI= -0.5

- Flux difference patterns are similar for El Niño, La Niña, and neutral phases.
- Large regional differences over land are predominantly caused by sampling differences due to uneven seasonal coverage of RAPS data used to develop the two sets of ADMs.

SW flux differences from these two sets of ADMs show no dependence on the ENSO phase

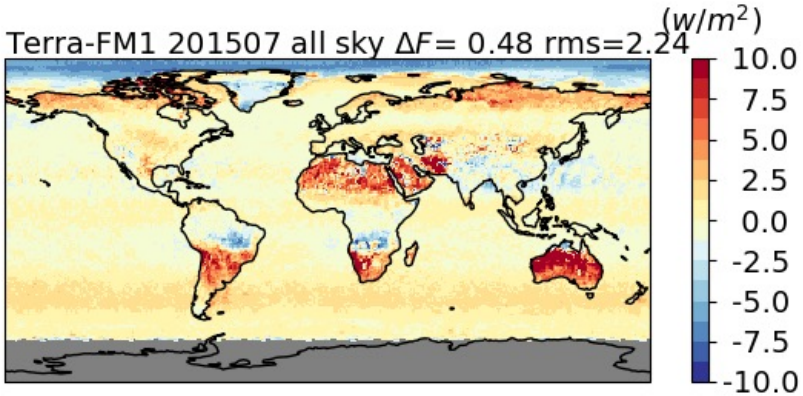

MEI= 1.7

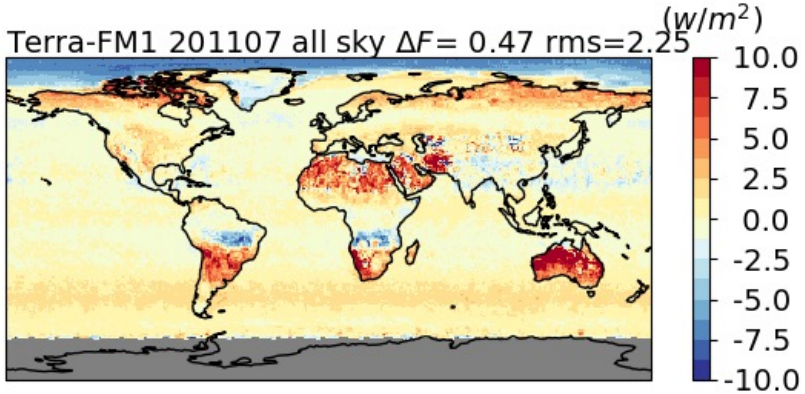

MEI= -0.9

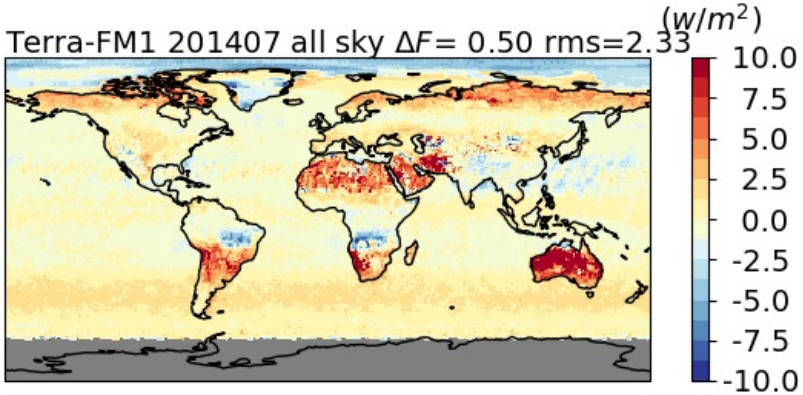

MEI= 0.3

- Flux difference patterns are similar for El Niño, La Niña, and neutral phases.
- Large regional differences over land are predominantly caused by sampling differences due to uneven seasonal coverage of RAPS data used to develop the two sets of ADMs.

SW flux variance analysis for different fresh snow ADM models

- For each ADM model and at a given SZA, the standard deviation of the fluxes can be used to assess the performance of ADMs.
- Apply La Niña ADMs and El Niño ADMs to an El Niño month and a La Niña month, then calculate the difference in relative standard deviation from these two sets of ADMs.

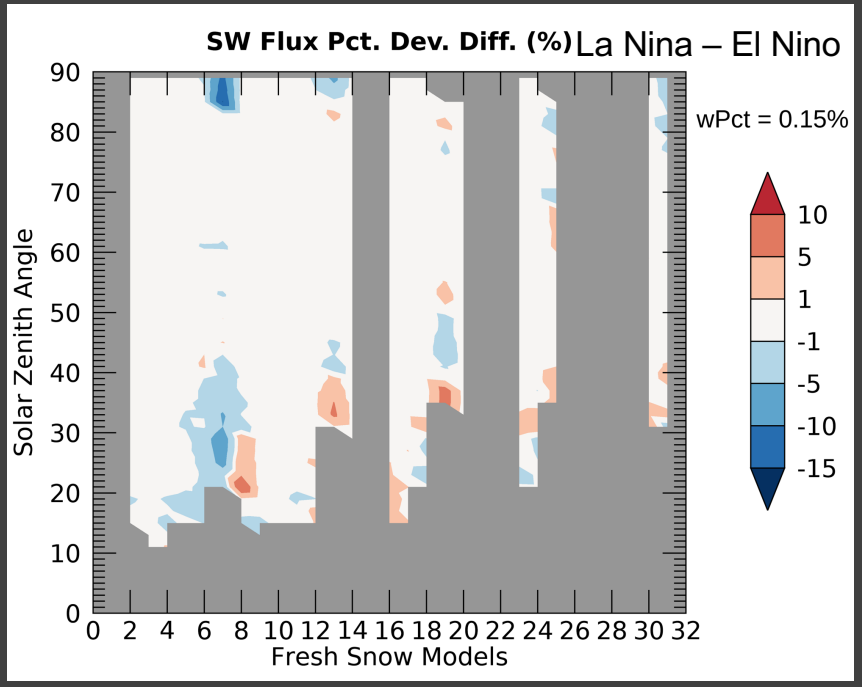

La Niña Months

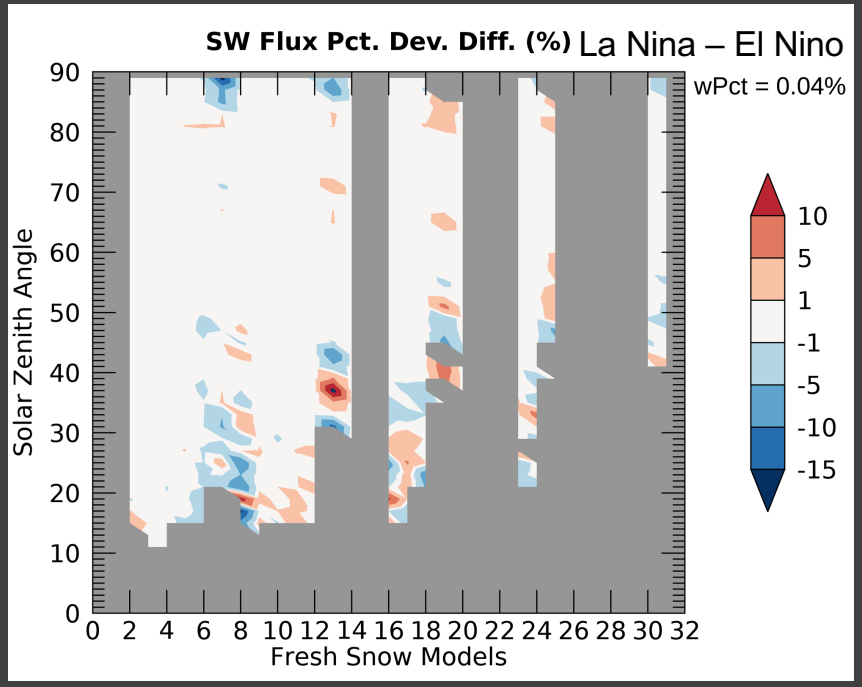

El Niño Months

For a CERES footprint, MISR provides spectral radiance measurements from nine camera angles

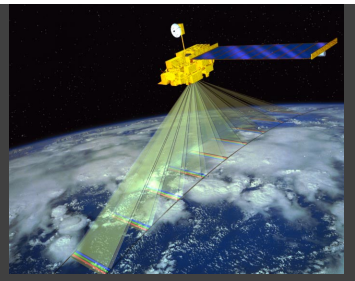

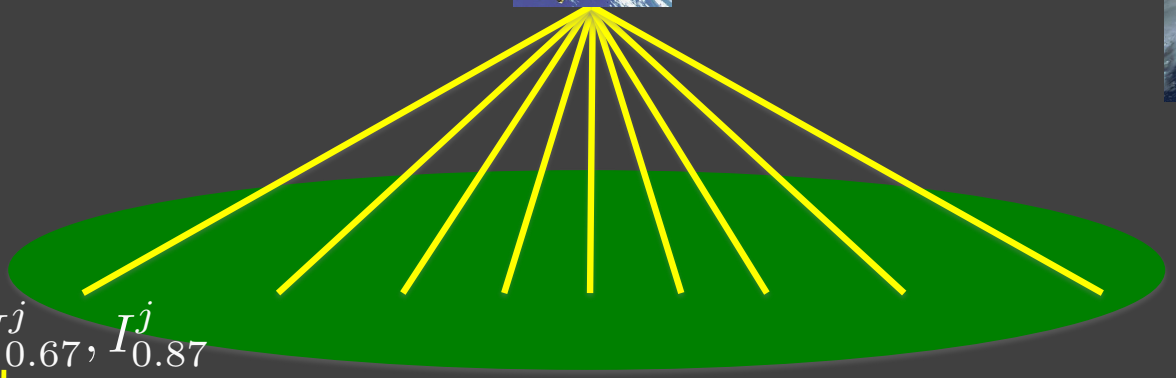

$$I^j_{0.45}, I^j_{0.67}, I^j_{0.87}$$

$$I^j_{sw} = c_0 + c_1 I^j_{0.45} + c_2 I^j_{0.67} + c_3 I^j_{0.87}$$

$$I^j_{sw}$$

CERES ADM

$$F^j_{sw} \longrightarrow \overline{F_{sw}} = \frac{\sum_{j=1}^{9} F^j_{sw}}{9} \longrightarrow s = \sqrt{\frac{\sum_{j=1}^{n} (F^j_{sw} - \overline{F_{sw}})^2}{n-1}}$$

For M CERES footprints, we calculate the mean standard deviation:

$$\overline{\sigma} = \sqrt{\frac{\sum_{i=1}^{M} s_i^2}{M}}$$

and the overall relative consistency:

$$CV_T = \left(\frac{\sqrt{\frac{1}{M}\sum_{i=1}^{M} s_i^2}}{\frac{1}{M}\sum_{i=1}^{M} \overline{F_{sw}^i}} \right) \times 100\%$$

$$I^j_{sw} = c_0 + c_1 I^j_{0.45} + c_2 I^j_{0.67} + c_3 I^j_{0.87}$$

I^j_{sw} I^c_{sw}

CERES ADM

F^j_{sw} F^c_{sw} → $CV_{NB} = \left(\frac{\sqrt{\frac{1}{m}\sum_{i=1}^{m} (F^j_{sw} - F^c_{sw})^2}}{\frac{1}{m}\sum_{i=1}^{m} F^c_{sw}} \right) \times 100\%$

$$CV_{ADM} = \sqrt{CV_T^2 - CV_{NB}^2}$$

SW flux consistency using MISR measurements over snow/ice

SW Flux ADM Error	Clear	Single Cloud Layer	Multi-Cloud Layer	All
Ψ_{ADM} (%) (Ed. 4 snow/ice ADMs)	3.8	5.9	5.8	5.5
Ψ_{ADM} (%) (El Nino snow/ice ADMs)	4.9	6.4	6.2	6.1
Ψ_{ADM} (%) (La Nina snow/ice ADMs)	5.0	6.3	6.0	6.0

A new method to partition TOA SW fluxes into visible and near-IR fluxes

Visible ADMs for Libera

- Libera has a split-shortwave channel (NIR: 0.7-5 μm), in addition to the traditional shortwave (0.3-5 μm), longwave (5-50 μm), and total (0.3-100 μm) channels.
- Radiances in the visible band (0.3-0.7 μm) can be derived by subtracting split-shortwave radiances from shortwave radiances:

$$I_{VIS} = I_{SW} - I_{NIR}$$

- Determine F_{SW} from I_{SW} using Libera team's CERES S-NPP SW ADMs.
- The goal is to partition the SW flux into visible and NIR portion:

$$F_{SW} = F_{VIS} + F_{NIR}$$

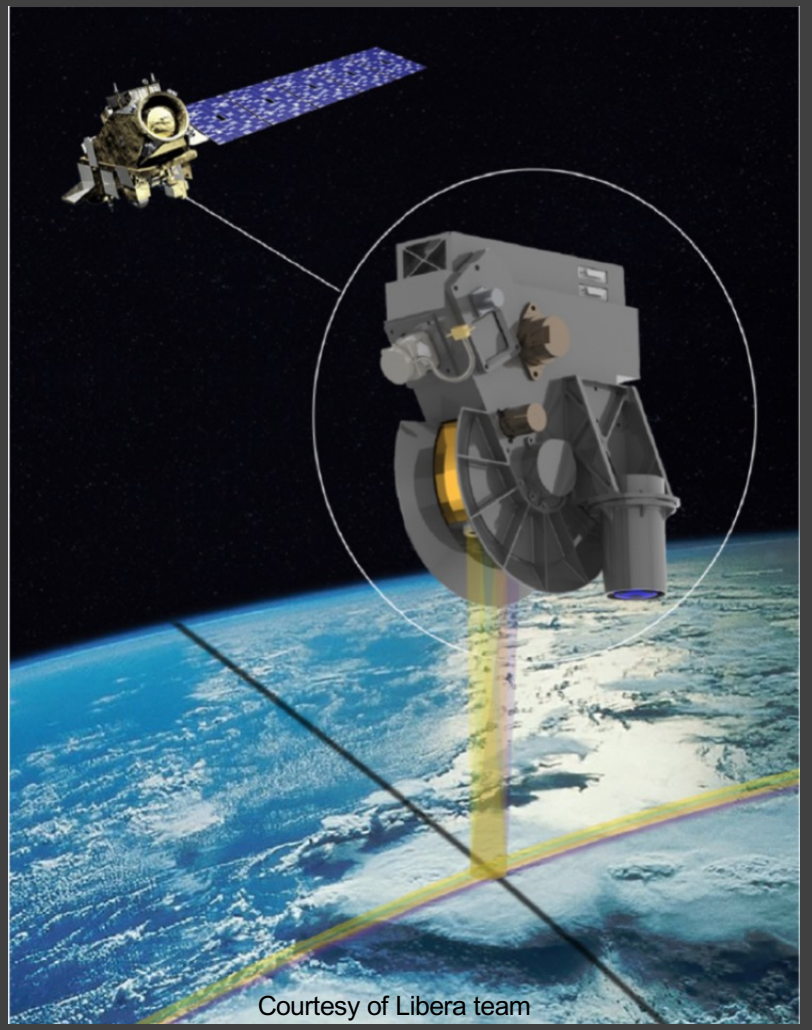
Courtesy of Libera team

Method to partition TOA SW fluxes into visible and near-IR fluxes

- Within each CERES footprint, the CERES team's VIIRS imager cloud algorithm provides the fractions of the footprint covered by clouds for up to two cloud layers.
- VIIRS spectral radiances are averaged over each cloud layer and the clear area if the footprint contains broken clouds.
- Calculate look-up-tables using MODTRAN for clear (including different aerosol types and optical depths) and cloudy (for different optical depth, size, and phase) conditions over different surface types.
- The MODTRAN LUTs include VIIRS spectral radiances at 0.488, 0.55, 0.640, 0.865, 1.24, 1.61, 3.74 um, and visible, NIR, and broadband SW radiances. Corresponding fluxes are also included.

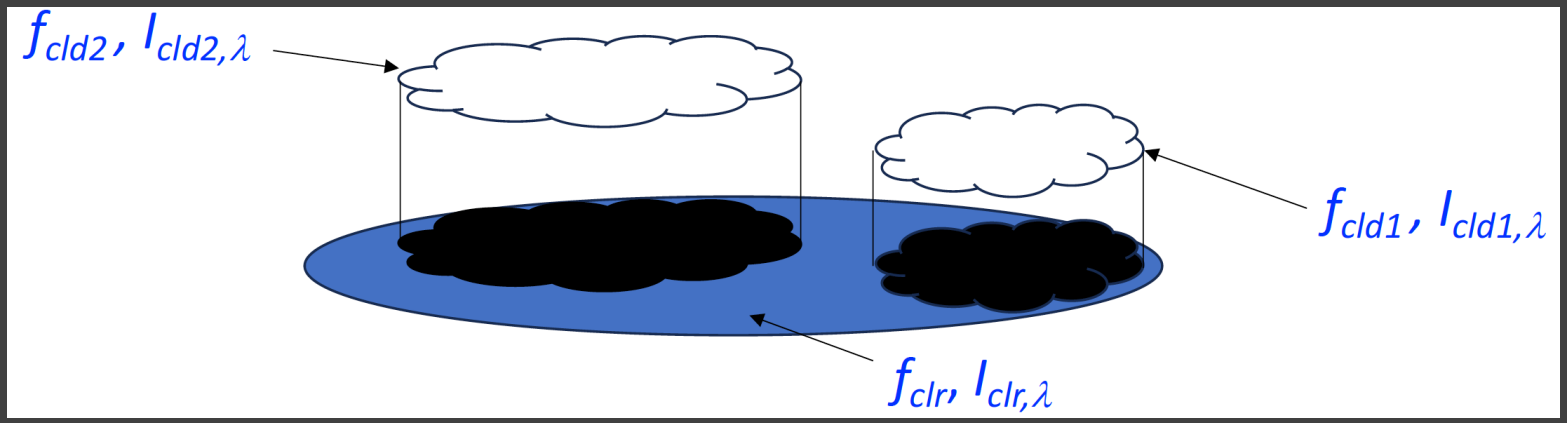

Method to partition TOA SW fluxes into visible and near-IR fluxes

- Select the MODTRAN simulations that best match the observed spectral radiances for each sub-footprint, then calculate the total footprint I'_{VIS}, I'_{NIR}, F'_{VIS}, F'_{NIR} by area-weighting sub-footprint values:

$$I'_x = [f_{clr} I'_{clr,x} + f_{cld1} I'_{cld1,x} + f_{cld2} I'_{cld2,x}]/(f_{clr} + f_{cld1} + f_{cld2})$$

$$F'_x = [f_{clr} F'_{clr,x} + f_{cld1} F'_{cld1,x} + f_{cld2} F'_{cld2,x}]/(f_{clr} + f_{cld1} + f_{cld2})$$

- Anisotropic factors for visible and NIR can be derived using I'_{VIS}, I'_{NIR}, F'_{VIS}, F'_{NIR} .

$$R_{VIS} = \pi I'_{VIS}/F_{VIS} \qquad R_{NIR} = \pi I'_{NIR}/F_{NIR}$$

- CERES instruments do not have NIR channel radiance measurements. The measured SW radiances is partitioned into visible and NIR portion by using the visible to SW radiance ratios derived from the LUTs for each footprint.

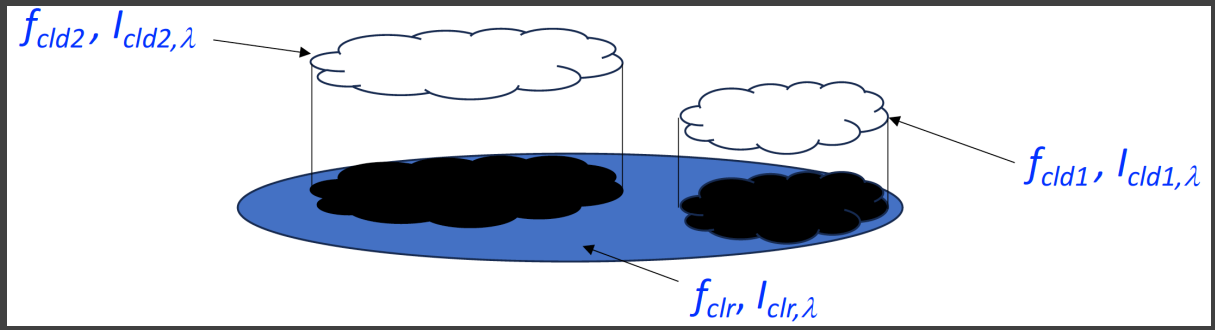

Instantaneous footprint level VIS, NIR and SW albedo: 20140101

- VIS, NIR, and SW albedo increase with COD until asymptote.
- VIS band has the highest albedo because cloud absorption is close to 0 for this band.
- NIR albedo is much lower than VIS due to cloud absorption.
- For high ice clouds, the difference between VIS albedo and NIR albedo is smaller than that for the low liquid clouds, mostly because ice clouds are more reflective, more so in the NIR band than the VIS band, and secondly because of reduced water vapor absorption above clouds.

Phase < 1.01; Height: 1-2 km; SZA: 30-60°

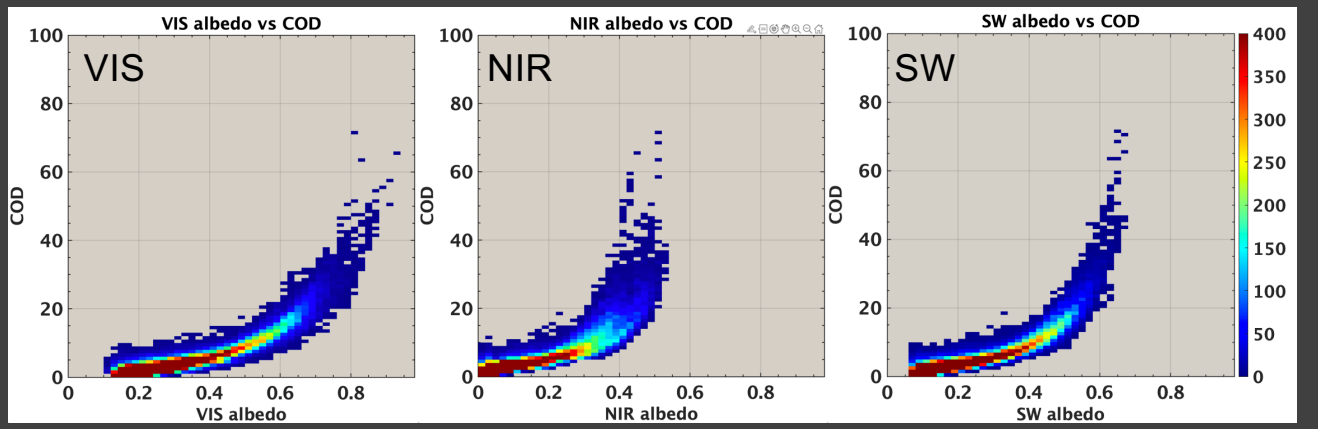

Phase > 1.75; Height: 5-10 km; SZA: 30-60°

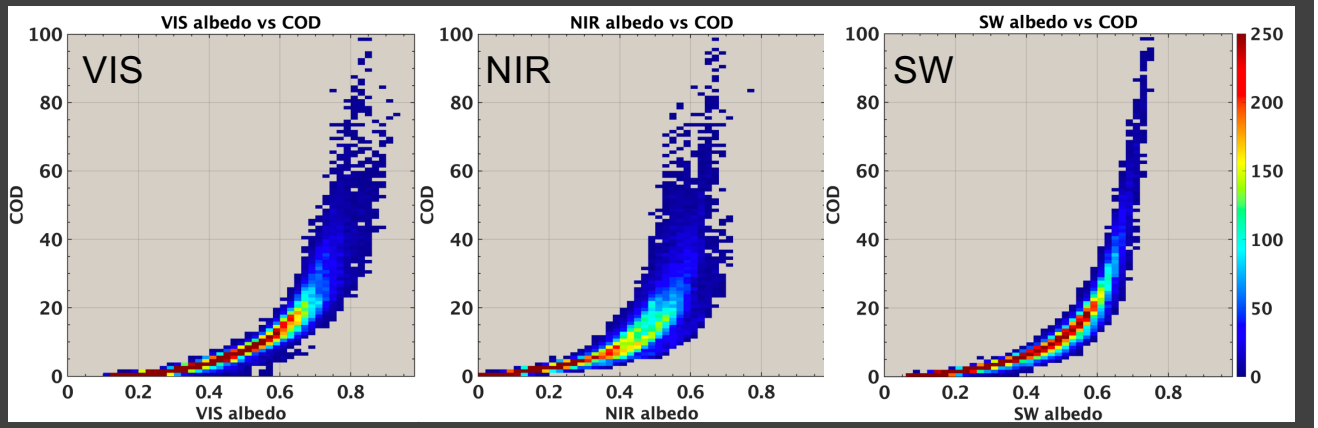

Monthly gridded instantaneous VIS and NIR albedo: 201401

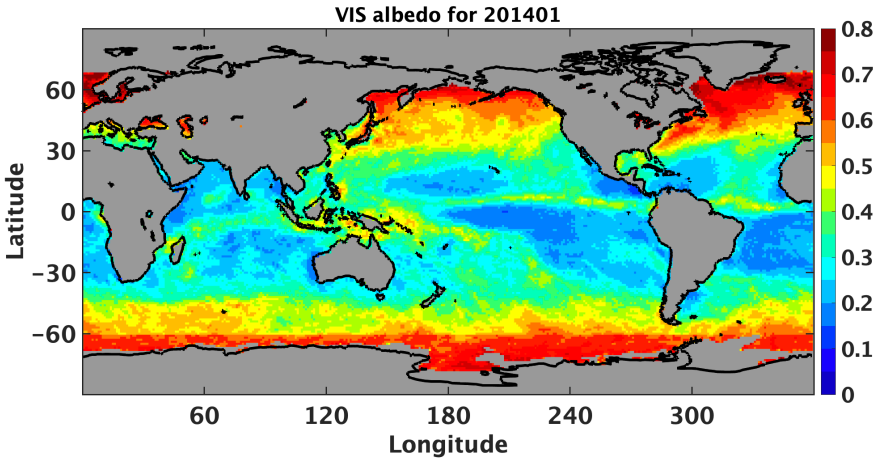

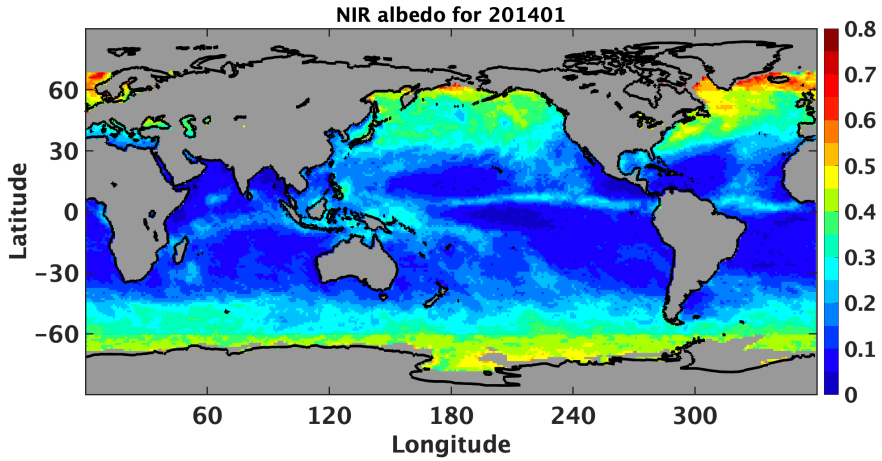

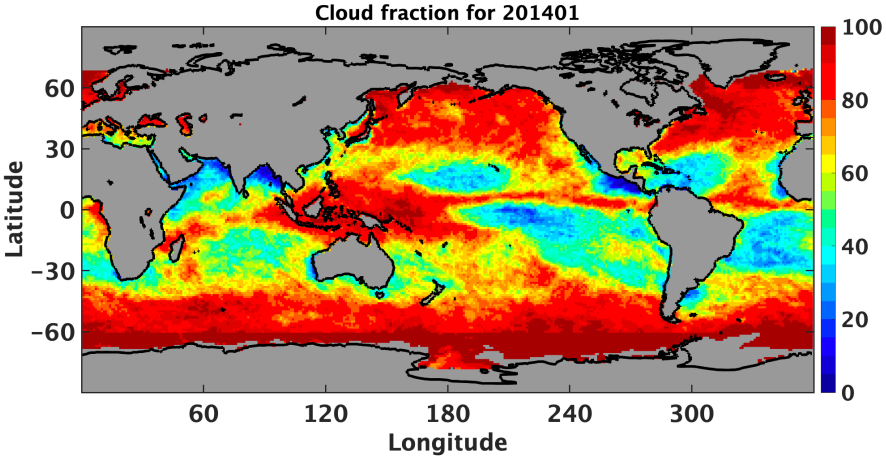

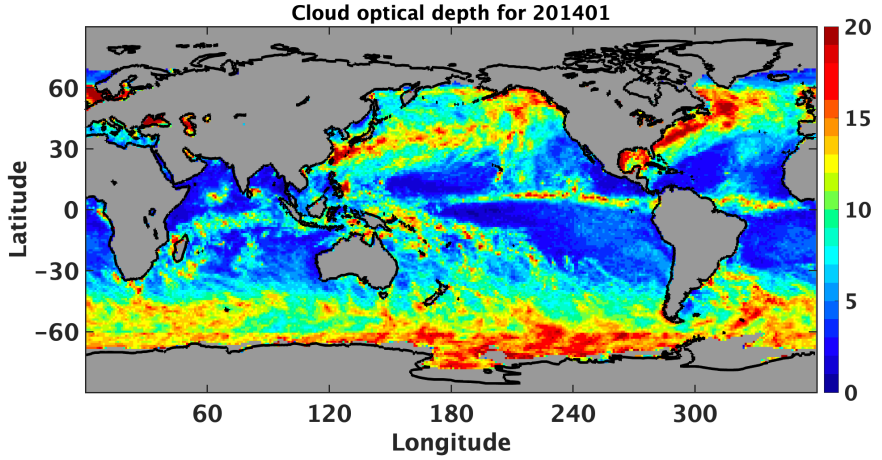

Relationship between shortwave albedo and NIR/VIS albedo ratio: 201401

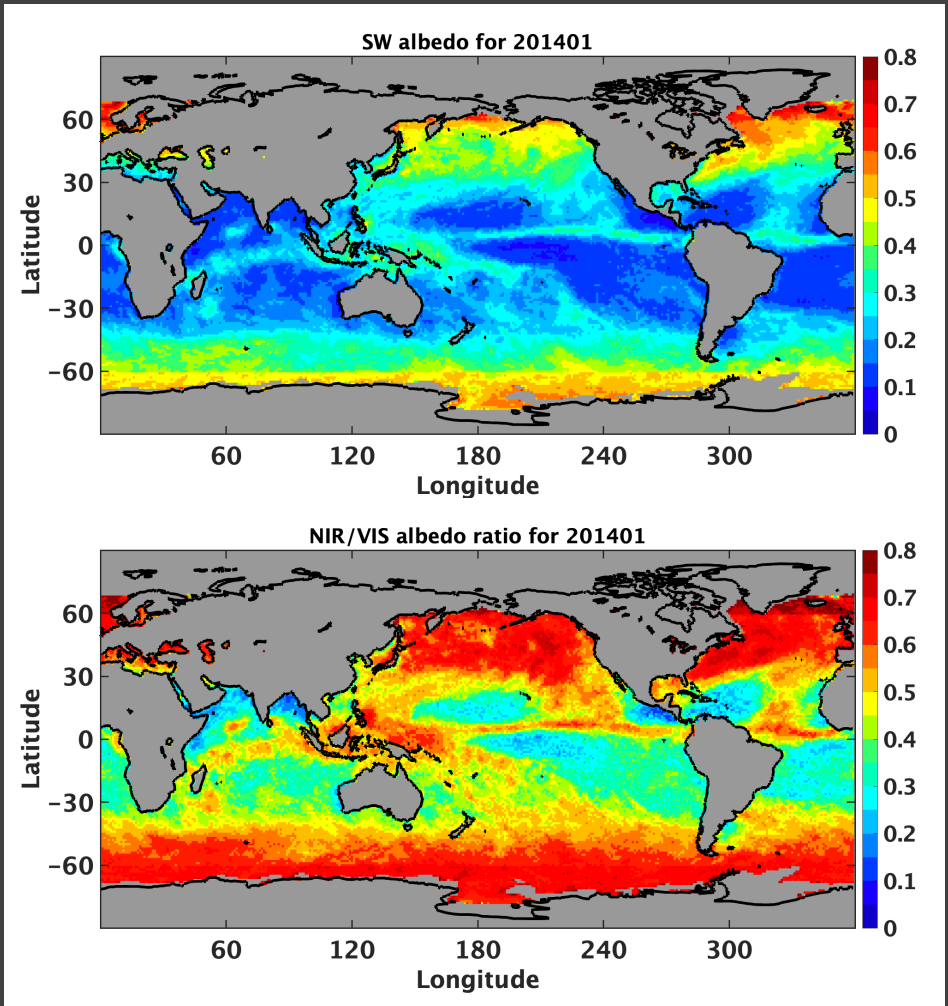

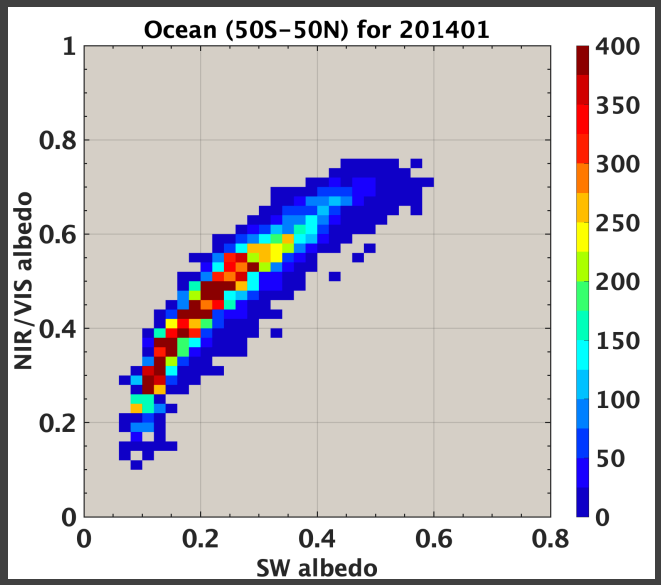

SW Albedo vs. NIR/VIS albedo ratio using gridded output from 50N to 50S ocean using four seasonal months of 2014 from S-NPP

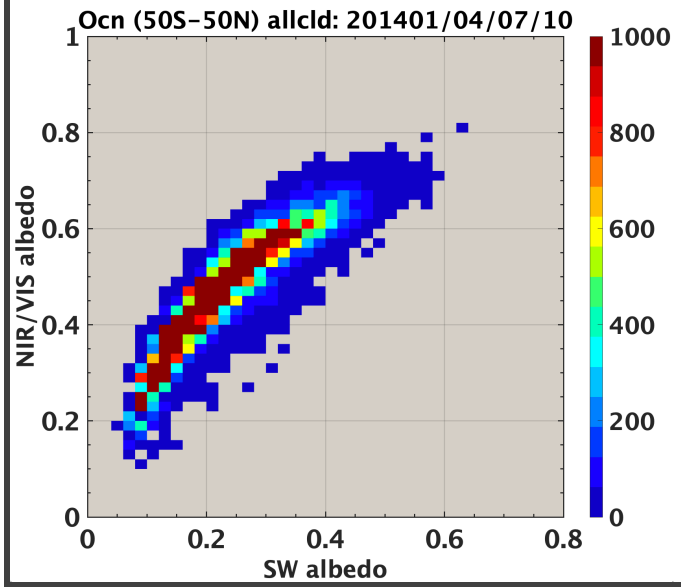

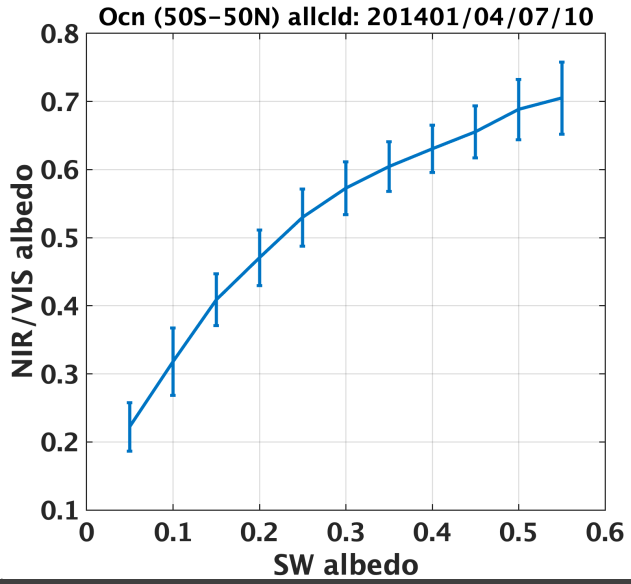

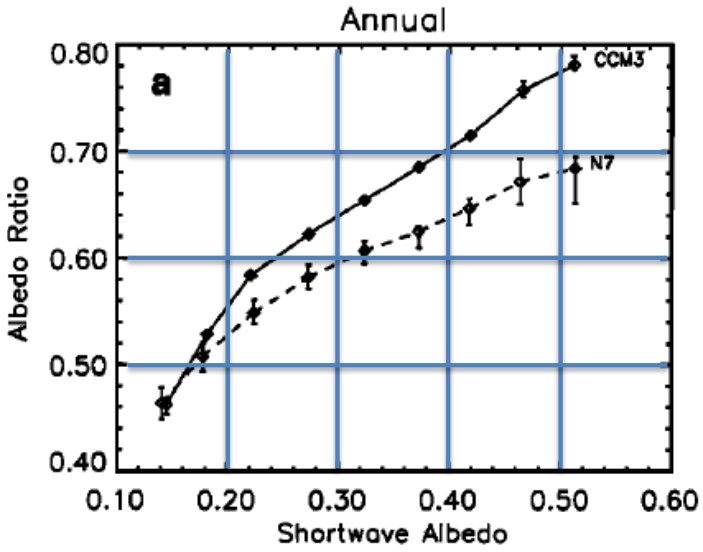

- The relationship from CERES is steeper than that from Nimbus 7.
- For SW albedo less than 0.4, NIR/VIS ratios from CERES are smaller than those from Nimbus 7.
- For SW albedo greater than 0.4, NIR/VIS ratios from CERES and Nimbus 7 are comparable.

From Collins (1998): Lines represent the mean ratio for ocean regions between 50S and 50N for 1979-1987. Vertical bars indicate the range of ratio computed for each individual year.

Visible and NIR albedo from SYN calculation

- CERES SYN contains calculated spectral fluxes. They are used to derive radiative transfer model-based VIS (0.43-0.69 μm) and NIR albedo.
- The model-based VIS and NIR albedo agree well with those that are derived using the partition method, adding confidence to the validity of the method that we developed.

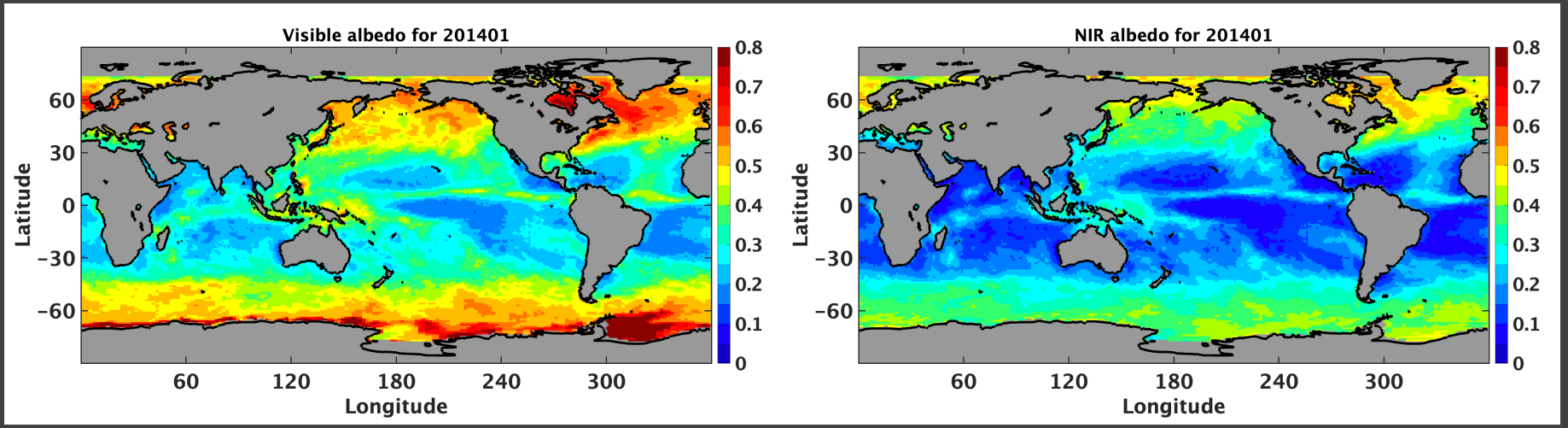

Summary

- Using data taken during different ENSO phases to test SW and LW ADM sensitivity to climate variability.
- LW ADMs constructed using data taken during El Niño phase and La Niña phase have a minimum impact on flux.
- SW fluxes inverted from El Niño and La Niña ADMs show consistent regional difference features that are independent of the ENSO phase of each month. These differences are predominantly caused by sampling differences due to uneven seasonal coverage of RAPS data used to develop the two sets of ADMs.
- Various consistency tests also indicate that the El Niño and La Niña ADMs have nearly the same uncertainty.
- Developed a new method to partition TOA SW fluxes into visible and near-IR fluxes.
- The relationship between SW albedo and NIR/VIS albedo ratio from CERES is steeper than that from Nimbus 7.
  - For SW albedo less than 0.4, NIR/VIS ratios from CERES are smaller than those from Nimbus 7.
  - For SW albedo greater than 0.4, NIR/VIS ratios from CERES and Nimbus 7 are comparable.